Transition of Linear to Exponential Hole Growth Modes in Thin Free-Standing Polymer Films

J. H. Xavier,* Y. Pu, C. Li, M. H. Rafailovich, and J. Sokolov*

Department of Materials Science and Engineering, State University of New York at Stony Brook, Stony Brook, New York 11794-2275

Received July 15, 2003; Revised Manuscript Received December 5, 2003

ABSTRACT: We have studied the formation and growth of holes in free-standing polystyrene films. For thick (~μm) films and sufficiently high temperatures, exponential hole growth vs time was observed. Using the theory of deBregeas et al. [*Phys. Rev. Lett.* **1995**, *75*, 21], relating growth rate to viscosity (η), we confirmed bulk scaling $\eta \propto MW^{3.2\pm0.2}$, where MW is the polymer molecular weight, and obtained good quantitative agreement with bulk viscosities. As temperature is lowered and/or films are made thinner, a transition to a linear growth mode of hole radius vs time is observed. The molecular weight dependence of growth velocity (V) for temperatures near the glass transition temperature (T_g) is $V \propto MW^{0.5\pm0.2}$. Our results also show an intermediate regime where growth is exponential, but bulk viscosities are not observed. Ellipsometry measurements, atomic force microscopy cross-section analysis, and optical images show no rim formation and uniform film thickening as holes grow.

Introduction

The stability of thin polymer films is a subject of considerable scientific and technological interest, with applications to coatings, adhesives, and lithography for electronic device fabrication. The polymers' viscous, elastic, and sometimes plastic response can all play a significant role in thin film breakup. For ultrathin films, where the bulk polymer radius of gyration R_g is comparable to or greater than the film thickness, changes in polymer conformations may cause large deviations from the bulk in dynamics and phase behavior. Also, relative to the relevant relaxation times, very high stain rates may be generated, permitting study of regimes of viscoelastic−plastic response not generally accessible in bulk measurements.

Previous work[1−14] has focused mainly on dewetting of polymers deposited on substrates, analyzing the rate of growth of holes and the shape of rims surrounding the growing holes. Recent theoretical work[11,15−19] has modeled the influence of strain rate dependent polymer response and surface capillary modes on film breakup and structure. Relatively little work has appeared on free-standing films,[20,21] the subject of this study. Debregeas et al.[20] studied thick (5−50 μm) films of poly(dimethylsiloxane) (PDMS) and observed that nucleated holes grew exponentially with time, accompanied by a uniform thickening (no rims) of the film outside the hole. They also developed a theoretical model, based on an energy balance equation including viscous dissipation and surface energy terms, which accounted for the exponential growth law of the hole radius, giving

$$r(t) = r_0 \exp(t/\tau_{flow}) \quad (1)$$

$$\tau_{flow} = \eta e/\gamma \quad (2)$$

where $r(t)$ is the hole radius at time t, r_0 is initial hole radius, η is the viscosity, e is the film thickness, γ is the surface tension of the polymer (the driving force for the hole growth), and τ_{flow} is the time for the hole radius to grow by a factor e.

Initially, our aim is to confirm the molecular weight dependence for thick PS films exhibiting the bulk scaling $\eta \propto MW^{3.4}$. Second, we studied thinner films at low temperatures, near T_g, where linear growth rates were found. Third, we measured the crossover between linear and exponential growth laws which occurs in the viscoelastic response of the films at intermediate temperatures, molecular weights, and thicknesses.

Table 1. Characteristics of Polystyrene Used for This Study

MW (g/mol)	R_g (Å)	M_w/M_n	MW (g/mol)	R_g (Å)	M_w/M_n
65K	71	≤1.04	200K	124	≤1.06
90K	83	≤1.04	270.5K	144	≤1.08
123K	97	≤1.08	650K	224	≤1.06
162.4K	112	≤1.05			

Experimental Procedure

Free-Standing Film Preparation. Monodisperse polystyrenes (PS) were purchased from Pressure Chemical for this project. Samples were prepared with PS of different molecular weights (MW) ranging from 65 kg/mol to 2 mg/mol. The radius of gyration of the polymer (R_g) and polymerization index of the samples are shown in Table 1. PS with various concentrations was dissolved in toluene, and solutions were filtered with a 10 cm^3 syringe (0.2 μm pore size filter). Films were spun-cast onto clean silicon wafers using a speed of 2500 rpm for 30 s. Ellipsometry was used to measure thickness of samples less than 0.5 μm thick and atomic force microscopy (AFM) for thicker samples (by scratching through the polymer sample down to the substrate and measuring the depth of the scratch). To prepare free-standing films, solutions were spun-cast onto a clean microscope glass slide, floated onto a distilled water bath, captured across a polished aluminum or silicon substrate with a 9 mm diameter hole at its center, and dried in air, as shown in Figure 1. To eliminate wrinkles in the films and flatten the surface after being deposited onto the substrate, the films were annealed at 120 °C for 30 min for samples ≥1 μm thick or 100 °C for 30 min for thinner samples under vacuum of 10^{-6} Torr. This step also removed any residual solvent molecules in the films. Optical microscopy was used to check for the presence of dust particles or imperfections in

* Corresponding authors: Tel 631-632-8483, Fax 631-632-5764, e-mail jxavier@ic.sunysb.edu, jsokolov@ms.cc.sunysb.edu.

10.1021/ma034999x CCC: $27.50
Published on Web 01/16/2004

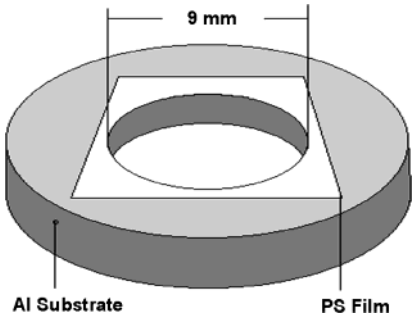

Figure 1. Geometry of free-standing PS film deposited on a 9 mm Al ring substrate.

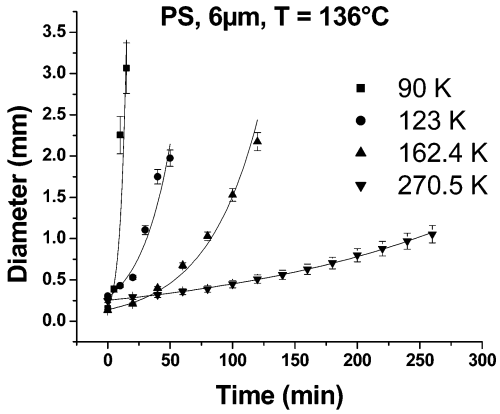

Figure 2. Exponential hole growth diameter vs time for PS films at $T = 136$ °C, film thickness (e) = 6 μm, and MW ranging from 90K to 270.5K.

the films. Nomarski phase contrast imaging was used to study the changing thickness of the films as the hole grows.

Hole Growth Experimental Setup. The hole growth experimental setup is composed of an Olympus optical microscope with video camera and a high-vacuum oven with a base pressure of 10^{-6} Torr. A temperature stability of ±0.5 °C was achieved using an Omega CN9000A proportional integral derivative (PID) temperature controller. For high-temperature experiments, such as $T \geq 120$ °C, the flow time (τ_{flow}) of the experiment was too short to simply insert a cold (room temperature) sample and holder into the oven. The PID temperature controller could not stabilize the temperature quickly enough, and no valuable data were able to be recorded. To solve this problem, we added an additional oven stage to preheat the films. The preheated oven temperature was set to 10 °C less than the experimental oven's temperature. To measure the hole growth mode of the free-standing films, a 50−100 μm diameter hole was nucleated in the center of the films using a clean sharp needle. No adhesion between the films and the needle was observed. After preheating, the nucleated holes were round and with uniform edge. To reduce the effect of the outer edges of the sample holder on the opening kinetics, we observed hole growth only up to ≈2.5 mm for 9 mm diameter samples. Using this technique, one can in principle investigate the viscoelastic response of polymer thin films. With a video camera, we observed the hole opening and measured its diameter as a function of time. Atomic force microscopy (AFM) was used to study the morphology of the film around the growing hole. Optical microscopy was also used to provide information on the morphology of the sample as the hole grows.

Results

In Figure 2, we plot the diameter of holes in the PS films as a function of time at $T = 136$ °C for thickness (e) = 6 μm and MW ranging from 90K to 270.5K g/mol. As seen from this plot, we observe an exponential hole growth of diameter with time for each MW, which can

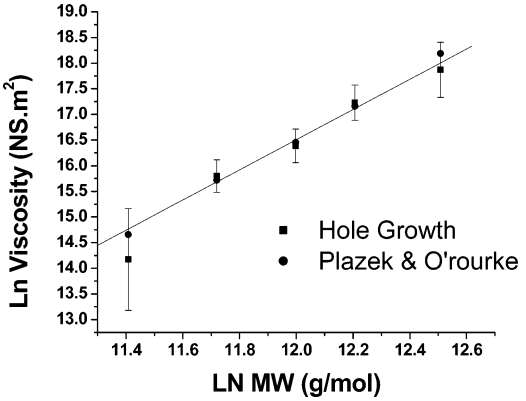

Figure 3. Plot of ln viscosity vs ln MW. PS films at T = 136 °C, film thickness (e) = 6 μm, and MW ranging from 90K to 270.5K. Hole growth (■), $\eta \propto MW^{3.2\pm0.2}$. Bulk, WLF (●), $\eta \propto MW^{3.4\pm0.0.2}$ (ref 23).

Table 2. PS (e = 6 μm, T = 136 °C, γ = 32.3 × 10^{-3} N/m)

MW (g/mol)	τ_{rep} (s)	τ_{flow} (s)	$\eta_{app} = \tau_{flow}\gamma/e$ (NS/m²)	η_{bulk} (NS/m²)
90K	492	265	1.43×10^6	2.32×10^6
123K	1271.5	1351	7.27×10^6	6.71×10^6
162.4K	2986.67	2445	1.31×10^7	1.4×10^7
200K	5491	5635	3.04×10^7	2.84×10^7
270.5K	13824	10714	5.77×10^7	7.92×10^7

be well described by eq 1. The slope of the curve is the hole velocity (V) with $\eta = \tau_{flow}\gamma/e$ and $\gamma = 32.3 \times 10^{-3}$ N/m.[22] The dynamics is dominated by the viscous dissipation, as explained in ref 20. To compare to the result for bulk polymers, $\eta \propto MW^{3.4}$, we plot ln η as a function of ln MW in Figure 3. We obtain a linear fit with slope 3.2 ± 0.2. An average of four experiments were done with the same set of samples, and the hole velocity values were reproducible within an experimental uncertainty of 10%. Within experimental error, we confirm the molecular weight dependence of bulk viscosity using eqs 1 and 2 of deBregeas et al.[20] We also note, as shown in Table 2, good *quantitative* agreement between our calculated viscosities and the literature values.[23] For these thick films at T well above T_g, $\tau_{flow} \sim \tau_{rep}$ (see Table 2), and the flow is bulk-liquid-like. However, as shown below, when $\tau_{flow} \ll \tau_{rep}$, the behavior is qualitatively different.

Next, we studied the hole growth in thinner films (800 → 5040 Å) at the temperature of the bulk glass transition, T_g, 100 °C. As shown in Figures 4 and 5, we found a clear linear hole growth rate at $T = 100$ °C as a function of time for PS, 200K, with $R(t) = R_0 + Vt \equiv R_0 + (1\text{ mm} \times t)/\tau_{flow}$, where R_0 is the initial hole radius at time $t = 0$, and we define a τ_{flow} for samples having a linear hole growth mode by $\tau_{flow} = 1$ mm/V. In contrast to the exponential regime, samples in the linear regime have a velocity that is independent of R_0, as shown in Figure 6. To illustrate the effect of molecular weight, we show in Figure 7 a plot of ln velocity as a function of ln MW. We find $V \propto 1/MW^{0.5\pm0.2}$ for $e = 2000$ Å, T = 100 °C and $V \propto 1/MW^{0.6\pm0.3}$ for the e = 800 Å, T = 100 °C set of data. These results show an intermediate regime between the purely viscous regime ($V \propto 1/MW^{3.4}$) and the purely elastic regime where velocity would be independent of molecular weight. (We also observed, as can be seen in Figure 5, a small oscillation superposed on the linear growth. This appears to be due to the effect of hydrodynamic wave modes present in the films, as discussed by Ferreiro et al.[24] in relation to their

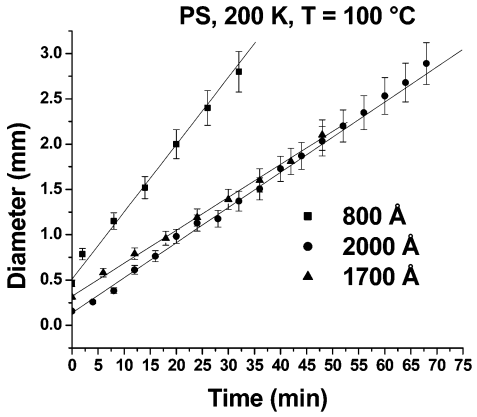

Figure 4. Hole diameter vs time. Linear hole growth for film thickness (e) ranging from 800 to 2000 Å for PS, 200K, and $T = 100$ °C.

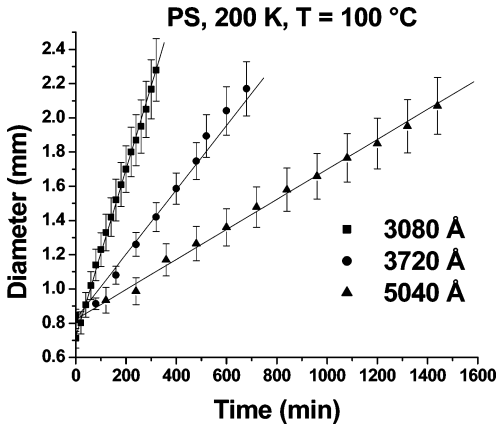

Figure 5. Hole diameter vs time. Linear hole growth for film thickness (e) ranging from 3080 to 5040 Å.

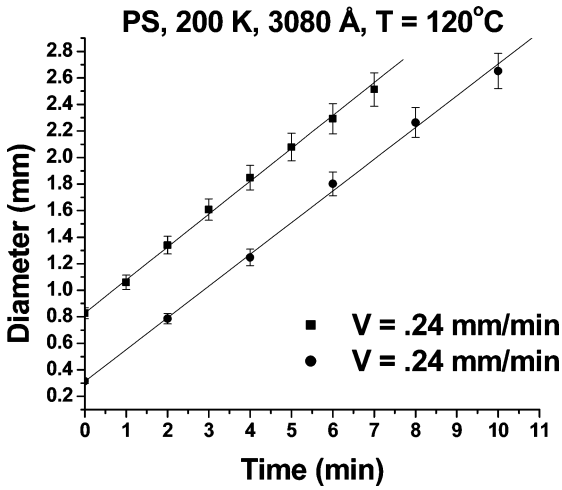

Figure 6. Hole diameter vs time. Linear hole growth with velocity independent of initial radius R_0.

observations of similar oscillations present in the growth rates of dendrites in polymer blends containing a crystalline component. In this paper, we do not consider this effect further.)

Between the low-T linear growth regime and the high-T bulk regime there must be a transition region. To investigate the dynamics in this intermediate regime, we observed the hole growth for PS, with $e = 0.5$ μm, $T = 128$ °C, and MW ranging from 123K to 650K g/mol and for MWs 200K and 650K we varied T from 120 to 135 °C. As we can see in Figure 8, we found an

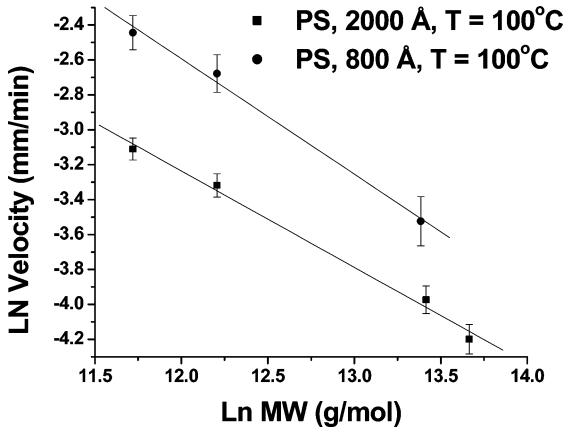

Figure 7. Plot of ln V vs ln MW of PS, $T = 100$ °C. Intermediate regime. For film thickness (e) = 2000 Å, $V \propto 1/\mathrm{MW}^{0.5\pm0.2}$. For film thickness ($e$) = 800 Å, $V \propto 1/\mathrm{MW}^{0.6\pm0.3}$.

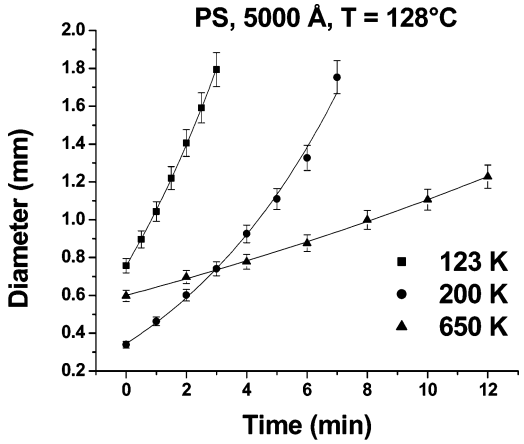

Figure 8. Hole growth diameter vs time in the transition region. PS films at $T = 128$ °C, film thickness (e) = 0.5 μm, and MW ranging from 123K to 650K.

exponential hole growth radius as a function of time for each MW. If eq 1 is used to calculate the viscosity (η) of the film for each experiment, the viscosity is not bulklike, being far lower than the bulk value. At this temperature, τ_{rep} is much greater than the τ_{flow} for these samples, and so the conditions for Brochard's theory to apply (relaxation of the elastic stress during the flow) are not valid here. We find that at $T = 120$ °C the hole radius grows linearly with time while from $T = 128$ °C to $T = 135$ °C the hole radius grows exponentially with time. For the $T = 128$ °C and $T = 135$ °C data in Figure 9, we multiply the time scale ($t = t_i \times 45/t_{final}$) to make the end points coincide, highlighting the differences in shape (linear vs exponential). This shows a crossover transition from linear to exponential hole growth at constant thickness and molecular weight. As temperature increases, the hole velocity increases while τ_{flow} and τ_{rep} decrease. Similar results were observed for PS, 650K, $e = 4980$ Å, as shown in Figure 10. In Figure 11, we plot ln velocity vs ln MW for PS, $e = 5020$ Å, $T = 128$ °C, where we find that $V \propto 1/\mathrm{MW}^{0.7\pm0.2}$. In this data set, the 2M PS showed linear growth while the lower molecular weights showed exponential growth (we take in those cases $V = 1$ mm/τ_{flow}). This result indicates an intermediate viscoelastic regime.

Finally, we show in Figure 12 a typical AFM image and cross sections of the region around the growing holes. Our data do not indicate a prominent, developing rim surrounding the holes as a function of time. Ellip-

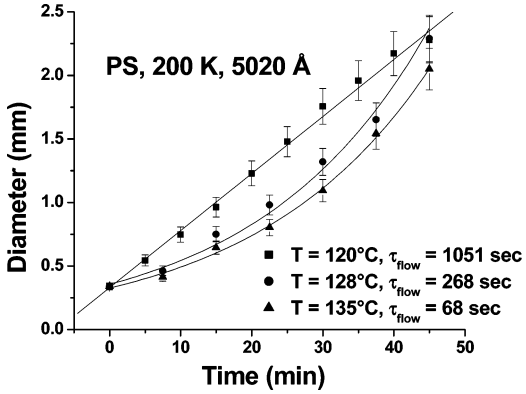

Figure 9. Hole growth diameter vs time. Transition from exponential growth to linear growth. PS, 200K, film thickness (e) = 5020 Å. For T = 128 °C and T = 135 °C, time and distance were scaled ($t = t_i \times 45/t_{final}$) to make end points coincide in order to show the differences in shape (linear vs exponential).

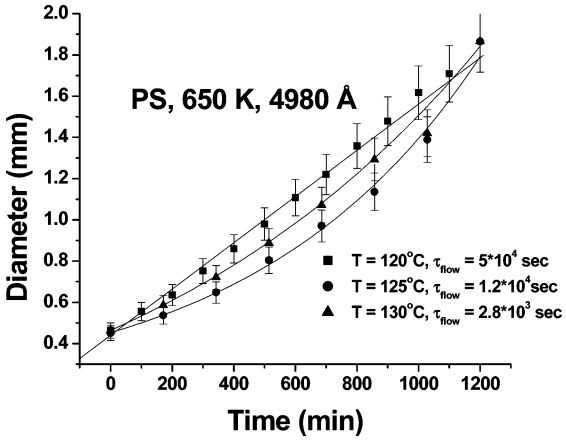

Figure 10. Hole growth diameter vs time. Transition from exponential growth to linear growth. PS, 650K, film thickness (e) = 4980 Å. For T = 125 °C and T = 130 °C, time and distance were scaled ($t = t_i \times 1200/t_{final}$) to make end points coincide in order to show the differences in shape (linear vs exponential).

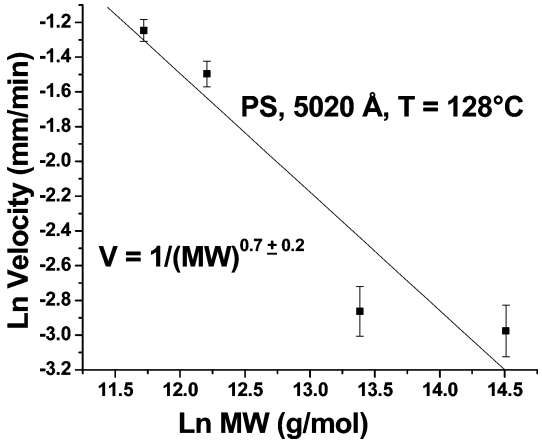

Figure 11. Plot of ln V vs ln MW. PS, film thickness (e) = 5020 Å, T = 128 °C. $V \propto 1/MW^{0.7\pm0.2}$; this result indicates an intermediate elastic regime.

sometry and Nomarski phase interference optical microscopy measurements show that the thickness of the film around the growing hole increases homogeneously, within experimental error. The issue of whether there is, or should be, a growing rim around the holes (where the material from the expanding hole would be deposited) deserves some comment. The previous two studies of free-standing polymer films[20,21] both reported an

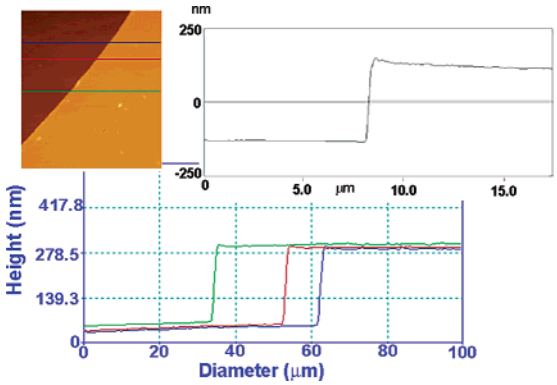

Figure 12. AFM cross section and image of a nucleated hole in a PS film, 200K, 1.725 mm, initial thickness = 2020 Å, thickness measured by ellipsometry = 2440 Å, thickness calculated assuming material from growing hole homogeneously redistributed through the remaining film = 2480 Å, film thickness from AFM cross section = 2400 Å. Ellipsometry measurements, AFM cross-section analysis, and optical images show uniform changes in film color and thickness as the hole grows.

absence of rims. In contrast, all previous studies on dewetting from substrates show rims.[25] Seemann et al.[11] and Herminghaus et al.[26] have shown that thin PS films dewetting from solid substrates exhibit pronounced oscillatory structures in the rim height profiles. Their hydrodynamic theory of the rim[11,26] predicts that these oscillations and the heights of the rims are reduced at high molecular weights such as those used in our experiments. It is possible that free-standing films have very small, broad rims that extend over most of the sample, though we do not believe this is the case. More work is needed to settle the matter.

Discussion and Conclusion

To assess the relative importance of viscosity, elasticity, and surface energy effects, we may estimate the different contribution to the energy balance. The simplest is the surface term:

$$\Delta E_{surface} = \pi[R^2(t) - R^2(t=0)] \times 2\gamma \qquad (3)$$

where $R(t)$ is hole radius at time t, γ is polymer surface tension, and $\Delta E_{surface}$ is the reduction in surface energy due to the hole growing to $R(t)$. Typical experimental values for our experiments are $R(t=0) \approx 0.2$ mm, $R(t) \approx 1$ mm, and $\gamma_{PS} \cong 35 \times 10^{-3}$ N/m, giving $\Delta E_{surface} \approx 2 \times 10^{-7}$ J, which number varies weakly over the studied temperature range. In the "bulk" high-temperature regime, where Brochard's theory[20] applies, this is balanced completely, to a good approximation, by the viscous losses $\Delta E_{viscous}$. The elastic contribution to the energy for radial flow is given by[27]

$$\Delta E_{elastic} = \mu \int (e^2_{rr} + e^2_{\theta\theta} + e^2_{zz})\, dV \qquad (4)$$

where μ is the elastic shear modulus and e_{rr}, $e_{\theta\theta}$, e_{zz} are the strain tensor components in cylindrical coordinates. If $\langle e^2_{ii} \rangle$ is the average value of e^2_{ii}, we have $\Delta E_{elastic} = \langle e^2_{ii} \rangle \mu V_{sample}$, with $V_{sample} = \pi R^2_{outer} e$. The shear modulus is time and temperature dependent, and we may use literature values[28] of the relaxation modulus $E_r(t)$ to estimate $\Delta E_{elastic}$. For 136 °C, we take $\mu \sim 10^3 \rightarrow 10^4$ Pa, and for $\langle e^2_{ii} \rangle \cong (1/10)^2$, $R_{outer} = 9$ mm, $e =$ 2000 Å, to obtain $\Delta E_{elastic} \sim 4 \times 10^{-10} \rightarrow 4 \times 10^{-9}$ J. This

is much smaller than $\Delta E_{surface}$ calculated above and indicates that Brochard's theory should work well here, as observed. For $T = 100$ °C, however, over experimental times of hours, the modulus falls into the plateau region, $\mu \sim 10^6$ Pa, and with other parameters as above we estimate $\Delta E_{elastic} \sim 4 \times 10^{-7}$ J, comparable to $\Delta E_{surface}$. Hence, the elastic part of the response cannot be ignored, a point which has been emphasized recently,[4,5,11,16,26] although it is clear that viscosity still plays the major role in limiting the growth velocity. (A model that only considers elastic and surface terms would give a velocity only limited by inertia effects, far higher than the observed velocities. In fact, the relevant velocity would then be the sound propagation velocity (~m/s), as discussed in Debregeas et al.[20] in relation to the propagation of elastic stress. Our observed velocities are 2−3 orders of magnitude lower than this at $T =$ 100 °C.) Since $t_{experimental} \sim \tau_{flow} \ll \tau_{rep}$, the effective viscosity is far lower than the zero shear rate limit and is deep into the shear rate dependent regime, as discussed by Danolki-Veress[21] and Carre et al.[29] Calculations of dewetting using rate dependent stress models have recently appeared, using the Wagner[18] and Cross models[19] and a viscoplastic theory.[17] However, these calculations do not consider an elastic contribution to the stress and lead to prominent growing rims developing around the advancing holes, in contrast to our experiments. The uniform thickening has been explained by deBregeas et al.[20] as due to a rapid (compared to τ_{flow}) elastic propagation of the Laplace pressure from the edge of the growing hole. An alternate explanation for the lack of a growing rim has been put forward by Brenner and Gueyffier,[30] using a viscosity-only model and the lubrication approximation for the Navier−Stokes equations. Their numerical results indicate that when the Stokes length υ/U_0 (υ is the kinetic viscosity, U_0 is the retraction velocity) is much smaller than the lateral dimensions of the film, then no rim develops. The absence of a rim in our experiments appears to be consistent with either explanation. Interestingly, Brenner and Gueyffier's results showed a linear growth law, but they attribute this to the fact that the calculations are two-dimensional. To date, no calculations have appeared that produce a linear growth mode in a circular geometry and without a growing rim.

As pointed out recently by Reiter,[4,5] yield phenomena may also be playing an important role in the dynamics near T_g (and even slightly above T_g since the time scales of the experiment are so short compared to the τ_{rep}). The system studied by Reiter in ref 4, thin PS layers on PDMS-coated Si wafers, is similar to the free-standing films studied here in the limit that PS−PDMS interfacial interactions can be ignored. The weak (or lack of) molecular weight dependence observed by Reiter is similar to our low-temperature results. However, the fact that sizable rims do develop around the growing holes in his samples indicates that the PS−PDMS interactions are significant and may explain why no clear linear growth regime was seen. Another factor may be that in the work of ref 4 many holes were formed spontaneously, and the presence of nearby holes can influence the growth rates.

We may note that the deformation resulting from a Laplace stress of γ/R ($\gamma =$ surface tension, $R =$ radius of hole) at the edge of a hole in an elastic membrane with elastic modulus μ is $U(R) = \gamma R/\mu e$.[20,27] Taking typical values in our experiments of $\gamma = 34.5 \times 10^{-3}$ N/m, $R = 0.25$ mm, $\mu \cong 10^6$ Pa, and $e = 2000$ Å gives $U(R) = 4.3 \times 10^{-5}$ m $= 43$ μm. That this is much less than the observed expansion of the growing holes to several millimeters in our films is a strong indication of plastic deformation. In Figures 13 and 14 we show the correlation between the ratio of the characteristic times τ_{rep}/τ_{flow}, and the ratio of the bulk viscosity to the apparent viscosity (calculated from eq 2). As expected, when τ_{rep}/τ_{flow} approaches one, the response becomes primarily viscous, values greater than one providing a quantitative measure of the deviation from viscosity-dominated behavior.

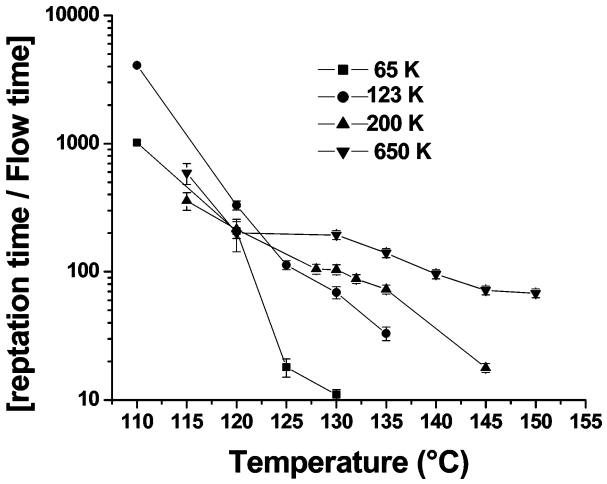

Figure 13. Bulk reptation time divided by flow time vs temperature for film thickness (e) ≈ 5000 Å and MW ranging from 65K to 650K.

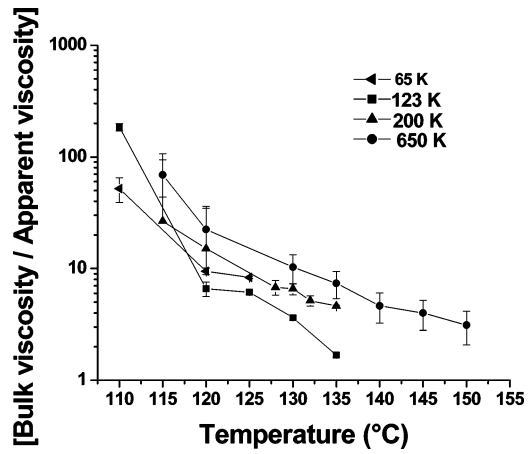

Figure 14. Bulk viscosity (ref 23) divided by apparent viscosity, $\eta = \tau_{flow}\gamma/e$ vs temperature for film thickness (e) ≈ 5000 Å, and MW ranging from 65K to 650K.

To conclude, we may say that a theory consistent with experiment near T_g must explain a linear growth law, absence of growing rims, and molecular weight dependence, $V \sim MW^{-0.5}$, intermediate between elastic-only, MW^0, and viscosity-only, $MW^{-3.4}$. We have argued that viscous, elastic, and plastic components of the stress all need to be considered. In very thin films, due to the driving force, surface tension, being independent of thickness, while the resistive forces are proportional to sample volume, very large strain rates (relative to typical relaxation times) are accessible compared to conventional bulk measurements, and we believe these experiments will help to develop an understanding of polymer dynamics in extremis.

Acknowledgment. We thank F. Brochard-Wyart, V. Shenoy, S. Safran, H. Mantz, and J. Douglas for enlightening discussions. Support of this work by the NSF MRSEC program (DMR 9632525) is gratefully acknowledged.

References and Notes

(1) Brochard-Wyart, F.; Daillant, *Can. J. Phys.* **1990**, *68*, 1084.
(2) Redon, C.; Brochard-Wyart, F.; Rondelez, F. *Phys. Rev. Lett.* **1991**, *66*, 715.
(3) Reiter, G. *Phys. Rev. Lett.* **1992**, *68*, 75.
(4) Reiter, G. *Phys. Rev. Lett.* **2001**, *87*, 186101.
(5) Reiter, G. *Eur. Phys. J. E* **2002**, *8*, 251.
(6) Martin, P.; Buguin, A.; Brochard-Wyart, F. *Europhys. Lett.* **1994**, *28*, 421.
(7) Lambooy, P.; Phelan, K. C.; Haugg, O.; Krausch, G. *Phys. Rev. Lett.* **1996**, *76*, 1110.
(8) Evers, L. J.; Shulepov, S. Yu. *Phys. Rev. Lett.* **1997**, *79*, 4850.
(9) Jacobs, K.; Herminghaus, S.; Mecke, K. R. *Langmuir* **1998**, *14*, 965.
(10) Jacobs, K.; Seemann, R.; Schatz, G.; Herminghaus, S. *Langmuir* **1998**, *14*, 4961.
(11) Seemann, R.; Herminghaus, S.; Jacobs, K. *Phys. Rev. Lett.* **2001**, *87*, 196101.
(12) Reiter, G.; Schultz, J.; Auroy, P.; Auvray, L. *Europhys. Lett.* **1996**, *76*, 1110.
(13) Reiter, G.; Sharma, A.; Casoli, A.; David, M. O.; Khanna, R.; Auroy, P. *Langmuir* **1999**, *15*, 2551.
(14) Masson, J.-L.; Green, P. F. *Phys. Rev. Lett.* **2002**, *88*, 205504.
(15) Herminghaus, S.; Jacobs, K.; Seemann, R. *Eur. Phys. J. E* **2001**, *5*, 531.
(16) Herminghaus, S. *Eur. Phys. J. E* **2002**, *8*, 237.
(17) Shenoy, V.; Sharma, A. *Phys. Rev. Lett.* **2002**, *88*, 236101.
(18) Saulnier, F.; Raphael, E.; de Gennes, P.-G. *Phys. Rev. Lett.* **2002**, *88*, 196101.
(19) Saulnier, F.; Raphael, E.; de Gennes, P.-G. *Phys. Rev. E* **2002**, *66*, 061607.
(20) Debregeas, G.; Martin, P.; Brochard-Wyart, F. *Phys. Rev. Lett.* **1995**, *75*, 3886.
(21) Danolki-Veress, K.; Nickel, B. G.; Roth, C.; Dutcher, J. R. *Phys. Rev. E* **1999**, *59*, 2153.
(22) Dee, G. T.; Sauer, B. B. *J. Colloid Interface Sci.* **1992**, *152*, 85.
(23) Plazek, D. J.; O'Rourke, V. M. *J. Polym. Sci., Part A-2* **1971**, *9*, 209.
(24) Ferreiro, V.; Douglas, J. F.; Warren, J.; Karim, A. *Phys. Rev. E* **2002**, *65*, 051606.
(25) Muller-Buschbaum, P. *J. Phys.: Condens. Matter* **2003**, *15*, R1549.
(26) Herminghaus, S.; Seemann, R.; Jacobs, K. *Phys. Rev. Lett.* **2002**, *89*, 056101.
(27) Landau, L. D.; Lifshitz, E. M. *Theory of Elasticity*, 2nd ed.; Pergamon Press: Oxford, 1970.
(28) Tobolsky, A. V.; Aklonis, J. J.; Akovali, G. *J. Chem. Phys.* **1965**, *42*, 723.
(29) Carre, A.; Eustache, F. *Langmuir* **2000**, *16*, 2936.
(30) Brenner, M. P.; Gueyffier, D. *Phys. Fluids* **1999**, *11*, 737.

MA034999X